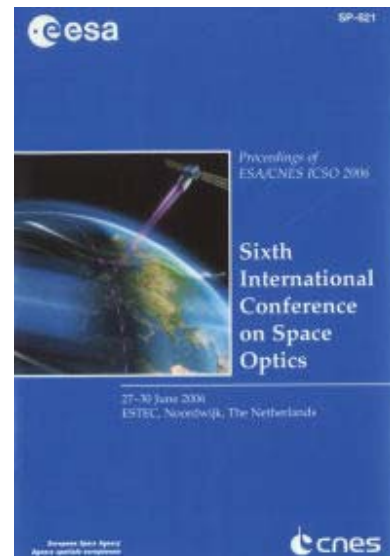


# International Conference on Space Optics—ICSO 2006

Noordwijk, Netherlands

27–30 June 2006

*Edited by Errico Armandillo, Josiane Costeraste, and Nikos Karafolas*



## *Simulation of reflecting surface deviations of centimeter-band parabolic space radiotelescope (SRT) with the large-size mirror*

*A. Kotik, V. Usyukin, I. Vinogradov, M. Arkhipov*



## Simulation of reflecting surface deviations of centimeter-band parabolic space radiotelescope (SRT) with the large-size mirror

A. Kotik<sup>1</sup>, V. Usyukin<sup>2</sup>, I. Vinogradov<sup>1</sup>, M.  
Arkipov<sup>1,2</sup>

<sup>(1)</sup> – Astro-space center of Physical Institute nm.  
Lebedev Russian Academy of Science, 84/32  
Profsoyuznaya st., 117997, Moscow, Email:  
kotik@asc.rssi.ru

<sup>(2)</sup> – Bauman Moscow State Technical University, 5, 2  
Baumaskaya st. 107547, Moscow, Email:  
rusengineer@mail.ru

### Abstract

The realization of astrophysical researches requires the development of high-sensitive centimeter-band parabolic space radiotelescopes (SRT) with the large-size mirrors.

Constructively such SRT with the mirror size more than 10 m can be realized as deployable rigid structures.

Mesh-structures of such size do not provide the reflector reflecting surface accuracy which is necessary for the centimeter band observations.

Now such telescope with the 10 m diameter mirror is developed in Russia in the frame of "SPECTR - R" program.

External dimensions of the telescope is more than the size of existing thermo-vacuum chambers used to prove SRT reflecting surface accuracy parameters under the action of space environment factors. That's why the numerical simulation turns out to be the basis required to accept the taken designs.

Such modeling should be based on experimental working of the basic constructive materials and elements of the future reflector.

In the article computational modeling of reflecting surface deviations of a centimeter-band of a large-sized deployable space reflector at a stage of his orbital functioning is considered.

The analysis of the factors that determines the deviations - both determined (temperatures fields) and not-determined (telescope manufacturing and installation faults; the deformations caused by features of composite materials behavior in space) is carried out.

The finite-element model and complex of methods are developed.

They allow to carry out computational modeling of reflecting surface deviations caused by influence of all factors and to take into account the deviations correction by space vehicle orientation system.

The results of modeling for two modes of functioning (orientation at the Sun) SRT are presented.

### Introduction

The integrated study of the SRT reflecting surface is the purpose of this work. This work is developed in the frame of "SPECTR - R" program: high-sensitive centimeter-band parabolic space radiotelescope for extra-large interferometer.

In mathematical model we took in to account:

Temperatures distortions;

Telescope manufacturing and installation faults;

The deformations caused by features of composite materials behavior in space.

The common space factor causing the distortions of the space structures is temperatures fields (Sun radiation). They are considered in computational modeling in an explicit form and allow us to model temperatures distortions.

The manufacturing and installation faults are also very important for telescopes with wave-length about 1 cm.

Mainly the SRT is made of composite materials. Their behavior features in space are caused additional deviations of the reflecting surface. These deviations are specific for the researching structure.

To take into account the manufacturing faults and behavior features of the composite materials in space we use the additional loads (moments, forces and enforced motions) in the model. Thus we consider all factors causing the deviations of the reflecting surface in the same model and can use finite-element method.

Telescope manufacturing and installation faults, and deformations caused by features of composite materials behavior in space aren't determinate.

Therefore the result deviations aren't also determinate.

To their analysis we use probabilistic model.

### Structure description

SRT has the parabolic reflector, his diameter is 10 meters.

It consists of the central part and 27 petals.

The petals are collapsed around SRT long axis (focal arm) at take-off phase.

The petal is laminate composite shell, fixed on the frame.

The frame consists of the longitudinal composite pipe and the transverse titanic ribs.

The reflector is placed in the Central Module (CM).

The transition arm connects CM with space service module.

### Finit-Elements Model

Software MSC.NASTRAN is used as a solver.

Brief model characteristic:

Nodes: 16122

Elements (Bar, Plate, Mass): 18301

General view of the FE model shows at the fig. 1.

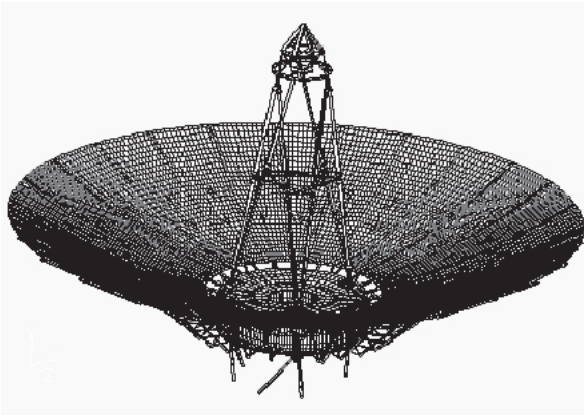


Fig. 1 FE model.

We verify the model by several tests:

- Test of the parasitic thermal stress of free model;
- Modal analysis of free model.

Beside these tests we made the numerical modeling of the petal deformation and comprised it with the results of the thermo-vacuum test [1].

**The analysis of the deviations.**

The normal deviations of the reflector surface are defined relative to 3 bases. These bases are:

The interface surface of the SRT and space service module. The deviations have additional constituent there. It is caused by rigid-body motions of reflector, which are the result of the temperature deformations of the central module and the transition arm.

The interface surface of the reflector and central module, where star sensors of orientation system are situated. In this case the rigid-body motions of reflector are excluded. Displacement of *i*-node in this case:

$$\{T\}_i = \{T\}_i^0 + \{X\}_i^0 - [\Omega] \cdot \{X\}_i^0 - \{\Delta\} \pm \{T_{ad}\}_i^0 \quad (1)$$

where

$[\Omega]$ - matrix of rotation;

$\{\Delta\}$  - vector of parallel displacement;

$\{X\}_i^0$  - nodal coordinates in global coordinate system;

$\{T\}_i^0$  - nodal displacement in global coordinate system;

$\{T_{ad}\}_i^0$  - additional vector, considering ground adjustment for example.

Best-fit paraboloid.

**Temperature deformations**

Because of the difficult form of the SRT antenna structure the definition of the temperature field is a difficult problem.

For the purpose of decreasing the temperature heterogeneity influence on the SRT function parameters of the petal frame pipes is using:

- For petal frame pipes the heater holds the  $-50...+50(C)$  temperature.

- For Central Module the heater and the heat pipes hold the  $+20(C)$  temperature.

We use the same finite element model as for the main problem decision (distortions of SRT mirror) as for temperature field calculation.

For the heat calculations we use the monolayer shell of the single petal. This monolayer shell has the effective thermophysical characteristics conforming to honeycomb structure ( $k_{eff} = 8 W/(m(C))$ ).

The effective heat conductivity along the frame pipes is  $35 W/(m(C))$  (composite with aluminum foil)

For other metal element we use the thermophysical characteristics from the technical guide.

The results of the direct measurements give us the thermo-optic characteristics of the petal shell for the calculation ( $A_s, \epsilon$ ):

for the reflector SRT work shell  $A_s = 0.6, \epsilon = 0.4$ ;

for the reflector SRT back shell (closed multi-level insulation - MLI)  $A_s = 0.4, \epsilon = 0.6$ .

To detect the thermophysical characteristics of MLI we use guide and define them more exactly using the results of thermo-vacuum tests of the petal [1].

We use the software TERM to define the external heat loads on SRT structure elements.

The cases of modeling for two modes of functioning (orientation at the Sun) SRT are studying:

- Load Set #1: "Sun is from below"
- Load Set #2: "Sun is from one side".

The main difference of these two variant is the temperature field of focal module arm.

Fig.2 is the results of the heat calculation for the single SRT petal. According to these results the petal shell temperature is located from  $-110$  to  $-140(C)$ , frame pipe temperature is located from  $20$  to  $-50(C)$ .

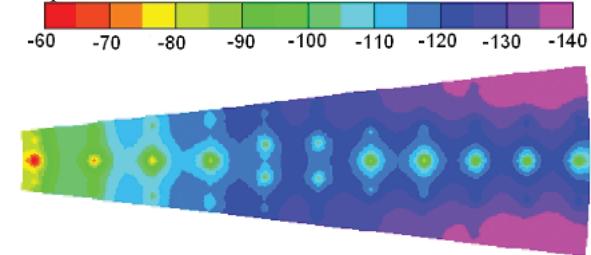


Fig. 2 Temperature field on the petal shell.

The Central Module temperatures, focal module temperatures and other structure elements are defining in similar way.

The view of the deformed model for Load Set 2 is shown at fig 3.

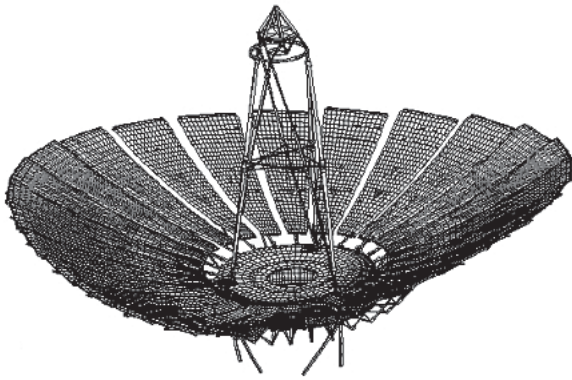


Fig. 3 The view of the deformed model for Load Set 2.

The field of the normal displacements (for Load Set 2) is shown at fig. 4 (in mm, the rigid-body motions of reflector are excluded) and fig. 5 (in mm, for best-fit paraboloid).

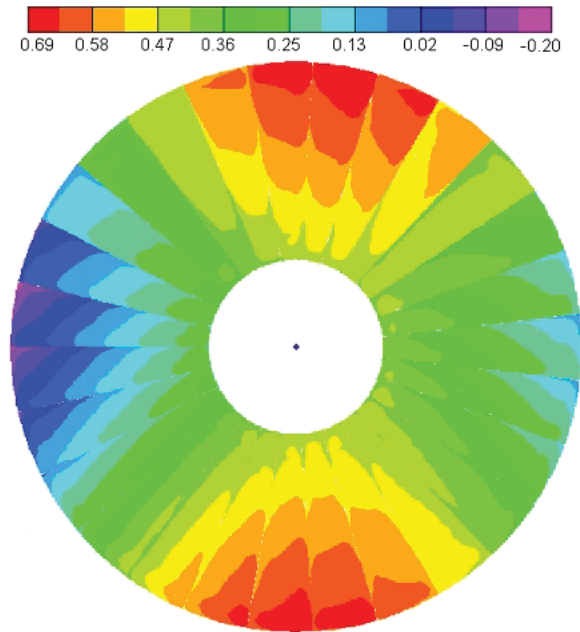


Fig. 4 The field of the normal displacements (in mm, the rigid-body motions of reflector are excluded, Load Set 2)

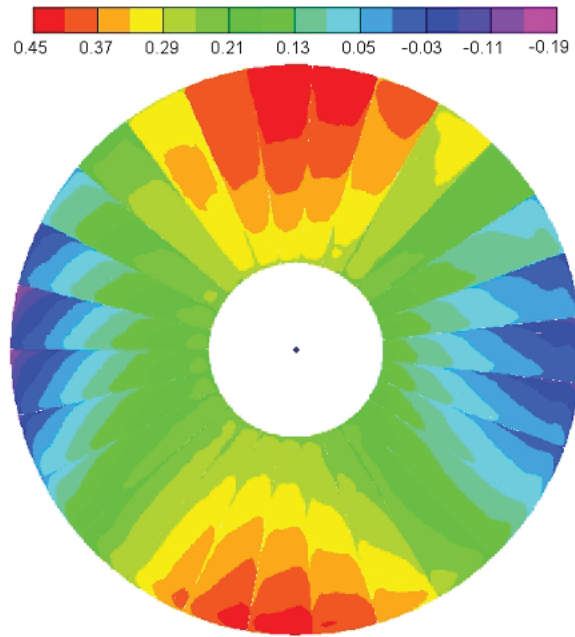


Fig. 5 The field of the normal displacements (related to best-fit paraboloid, Load Set 2).

**Manufacturing faults and the space influence**

The manufacturing and installation faults are important not determinate factor, influencing on the deviations from theoretic profile. The technological experiments with single detail allow us to define these faults. Maximum values of the faults are describing in the specifications. The space influence consists in sublimation of composite components. This sublimation reduces to additional shell distortions and bending and torsion of composite frame pipes. Such distortions are determined during the thermo-vacuum tests [1]. The couple of enforced motions (card SPC of MSC.Nastran), prescribed in join points shell/frame take into account the technical deviations in model ( $\pm T_n$ , fig. 6). The enforced motion values are changed random in interval, prescribed in technical specification.

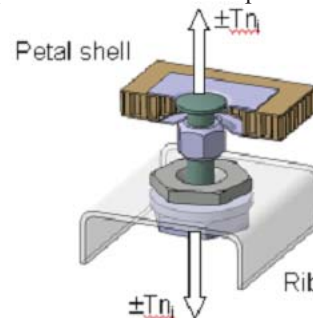


Fig. 6 The join points shell/frame and the enforced motion.

Such method allows getting the “smooth” deviation field. Special software is used for the MSC.Nastran input file creation. Load sets are created automatically

and added to the based MSC.Nastran input file. Input file contains 50 load sets. In each load set the enforced motion value for all join points shell/frame is changing. Typical distribution of the normal displacements (in mm) caused by manufacturing faults and the vacuum influence on the petal shell is shown at fig. 7.

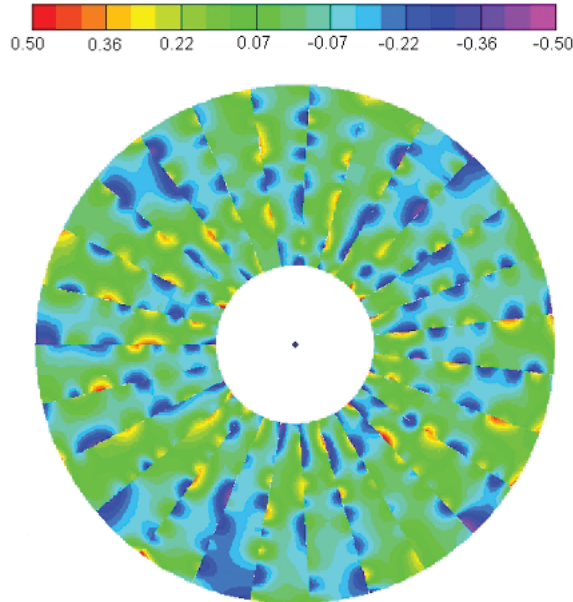


Fig. 7 The field of the normal displacements (the manufacturing and installation faults and the space influence).

Bending and torsion are used in the model as equivalent bending and torsion moments, applied at the end of the composite pipes of the frame (fig. 8).

The equal moment values are also changed random in interval, prescribed in technical specification. The technological experiments with single pipe allow us to define these angles of bending and torsion.

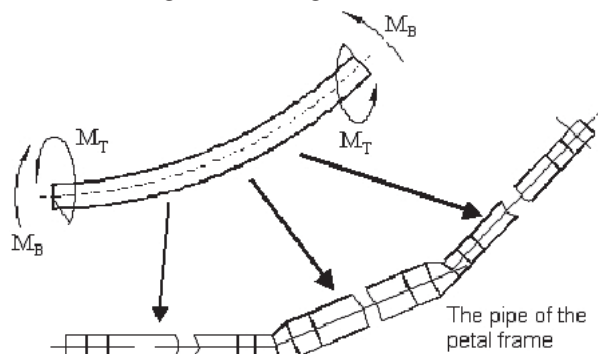


Fig. 8 The equivalent bending and torsion moments

Special software is used for the MSC.Nastran input file creation. Load sets are created automatically and added to the based MSC.Nastran input file. Input file contains 50 load sets. In each load set the bending and torsion moment value for all pipes for all frames is changing.

Typical distribution of the normal displacements (in mm) caused by vacuum influence on the frame pipes is shown at fig. 9.

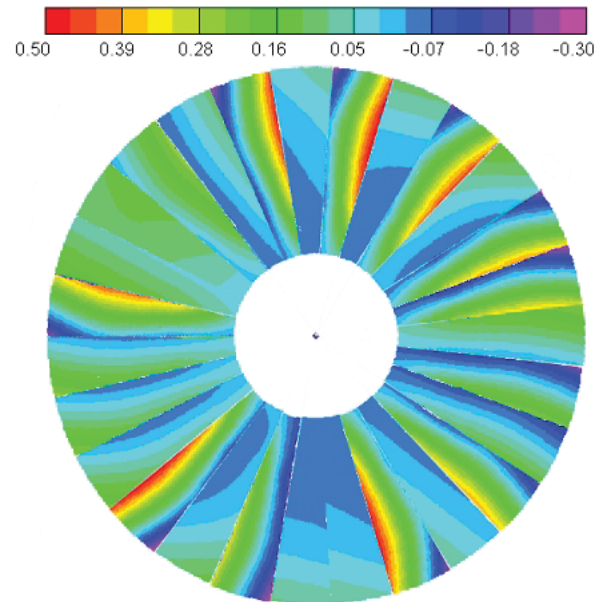


Fig. 9 The field of the normal displacements (the space influence on composite pipes).

**Result analysis**

Special software is developed to analyze reflecting surface deviations, caused by the complex of the deformation factors. This software uses the results of the numerical modeling get from MSC.Nastran (files \*.f06). It allows us to get the normal deviation fields at different bases (with exception of the rigid-body motion, relative to best-fit paraboloid, see fig. 3 and 4 for example) and carries out the probabilistic analysis of the deviations, caused by the all deformation factors. The distribution of the probability for normal deviations (caused by the all deformation factors for two orientation variants) is shown at fig. 9 and 10.

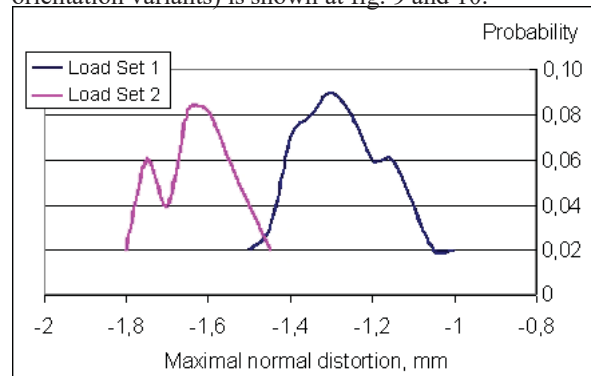


Fig. 9 The distribution of the probability for maximum normal distortions.

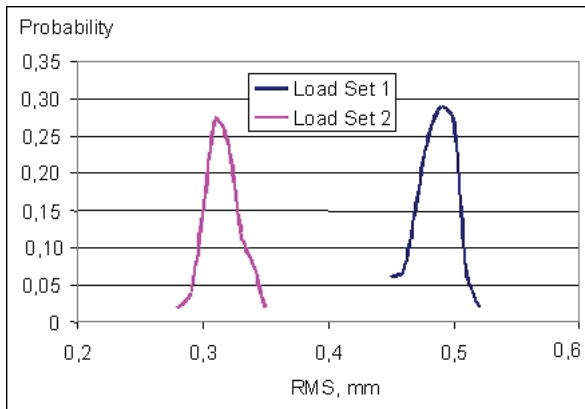


Fig. 10 The distribution of the probability for RMS distortions.

### Conclusion

- The complex analysis of the reflecting surface deviations is carried out.

### References

1. Radio Astron. Profile measurements on two modified Petals of the Space Radio Telescope Antenna. Thermocycling test in ESTEC – HBF-3. TOS-MTE/T/MET/0264, 1998.